

Composition of Saliency Metrics for Channel Pruning with a Myopic Oracle

Kaveena Persand¹ Andrew Anderson¹ David Gregg¹

Abstract

The computation and memory needed for Convolutional Neural Network (CNN) inference can be reduced by pruning weights from the trained network. Pruning is guided by a pruning saliency, which heuristically approximates the change in the loss function associated with the removal of specific weights. Many pruning signals have been proposed, but the performance of each heuristic depends on the particular trained network. This leaves the data scientist with a difficult choice.

We propose a method to compose several primitive pruning saliencies, to exploit the cases where each saliency measure does well. Our experiments show that the composition of saliencies avoids many poor pruning choices identified by individual saliencies. In most cases our method finds better selections than even the best individual pruning saliency.

1. Motivation

Channel pruning schemes can range from pruning all channels with their saliency below a predetermined threshold (Mao et al., 2017) to machine learning guided schemes (He et al., 2018b). Regardless of the pruning scheme chosen, some form of saliency metric is used to estimate the relative importance of different weights or sets of weights.

One of the most widespread heuristics used for channel pruning is to use the L1-norm of the weights as the saliency metric (Mao et al., 2017). In simple terms, the larger the mean weight value in a channel of the kernels, the more likely the channel is to be contributing to the result.

Other metrics aiming to more accurately predict channel saliency for pruning have been proposed, such as APoZ (Hu et al., 2016), the Fisher Information (Theis et al., 2018), and 1st Order Taylor expansions (Molchanov et al., 2017). All of these metrics use different *fixed* assumptions about the

relative magnitudes of weights, activations, and gradients.

When using any one saliency metric for the entire pruning process, we run the risk of the metric assumptions being invalidated, leading to poor decisions being made by the metric. Ideally we could combine the best aspects of different saliency metrics. However, despite an extensive literature review, we are unable to find any prior work on composing *different* saliency metrics. The chief difficulty lies in combining the numerical output of different saliency metrics, which are not directly comparable.

Contributions

No metric is *always* correct. We propose a method of combining the predictions of multiple saliency metrics which can avoid poor choices that are made by otherwise effective metrics. We use a set of *constituent* saliency metrics to create a shortlist of candidate channels for pruning. We evaluate each proposal with a *myopic oracle* to measure the deflection in cross-entropy loss that arises from actually pruning the given channels.

We make the following principal contributions:

- We demonstrate that different saliency metrics perform differently on different networks.
- We establish a way to combine different saliency metrics without any prior knowledge of the network via the myopic oracle.
- We perform an in-depth experimental investigation using a selection of different networks with state-of-the-art saliency metrics from prior work.

The remainder of this paper is structured as follows. Section 2 discusses the state of the art of pruning with saliency metrics. Section 3 discusses the issue of connectivity between pruned parameters. Section 4 describes our proposed method. Section 5 describes our experimental setup, and Section 6 contains our results. Section 7 concludes.

2. Background

Pruning reduces the size and computational cost of CNNs by reducing the number of parameters. Pruning strategies

¹Trinity College Dublin, Dublin, Ireland. Correspondence to: Kaveena Persand <persandk@tcd.ie>, Andrew Anderson <aanderso@tcd.ie>, David Gregg <david.gregg@cs.tcd.ie>.

attempt to find values within the weight tensors that can be replaced by zero with little impact on the accuracy of the CNN.

2.1. Granularity of Pruning

Pruning can be applied at different levels of granularity (Mao et al., 2017; Wen et al., 2016). The most fine-grain approach is to replace arbitrary individual weights with zero (Han et al., 2015). *Fine-grain* pruning can reduce the number of weight parameters by a large amount (Mao et al., 2017), but the resulting weight tensors have arbitrary patterns of zero and non-zero values that are difficult to exploit efficiently. *Structured* pruning removes regions of weights from the tensors, such as individual kernels (Li et al., 2017), or sequence of values.

In this paper we focus on coarse-grain pruning, where we prune entire output channels from the weight tensors of convolution layers.

Channel pruning has two significant advantages compared to pruning weights at a finer level of granularity. First, the resulting pruned weight tensors become smaller, but *do not* become sparse. It is therefore possible to use these smaller tensors with existing highly-tuned software that assumes dense tensors. Second, when an entire output channel is pruned from a convolution layer, the weights for the corresponding input channel in a subsequent layer become redundant and can also be pruned. Thus, there is a double effect on model size when pruning output channels.

2.2. Penalty Terms

The removal of weights from the network can be done using *penalty terms* (Reed, 1993). Penalty terms are typically used during the training process to introduce sparsity. Pruning using penalty terms can be simplified to a modification of the network’s optimization and cost functions to promote networks with fewer weights.

2.3. Saliency Metrics

Saliency metrics can also be used to prune weights. A *channel* saliency metric estimates which channels are least likely to affect the network’s accuracy when pruned. While early works on saliency metrics for pruning in neural networks focused on using fully trained networks (Mozer & Smolensky, 1988; Karnin, 1990; LeCun et al., 1989; Hassibi & Stork, 1992), recent work has shown that saliency metrics can successfully be used to remove parameters from the network at different stages of the training process (Frankle & Carbin, 2019; Lee et al., 2019).

In this paper, we focus on the use of saliency metrics for channel pruning.

Saliency metrics can be classified into two broad groups: static and dynamic saliency metrics.

2.4. Static Pruning Saliency Metrics

Static saliency metrics, consider only the values of the weights, and avoid the need to perform a forward pass of the network. Commonly used static pruning saliency metrics are the L1-norm of the weights (Mao et al., 2017) and the mean squares of the weights (Molchanov et al., 2017) (see Equation 1).

$$S(C_i) = \frac{1}{\text{card}(W_i)} \sum_{w \in W_i} w^2 \quad (1)$$

The L2 and L1 norm of the weights have been used in multiple pruning schemes (Lebedev & Lempitsky, 2016; Li et al., 2017; He et al., 2018a) for different granularities of pruning. Weights-based saliency metrics assume that weights of lower magnitude have a lower contribution to the network.

2.5. Dynamic Pruning Saliency Metrics

More recent work has proposed *dynamic* saliency metrics, which can exploit the information in the activations and gradients. These can only be obtained by performing a forward, and an additional backward, pass of the network, respectively.

2.5.1. ACTIVATION-BASED SALIENCY METRICS

Some examples of effective dynamic saliency metrics are the absolute-percentage-of-zeros (Hu et al., 2016), mean (Anwar et al., 2017) (Equation 2) and standard deviation of activations (Polyak & Wolf, 2015). Activation-based saliency metrics exploit information only obtainable during forward passes of the network.

$$S(C_i) = \frac{1}{\text{card}(A_i)} \sum_{a \in A_i} a \quad (2)$$

2.5.2. GRADIENT-BASED SALIENCY METRICS

Conversely we can find pruning saliency metrics that make use of only the gradients (Karnin, 1990) such as the use of the average of the gradients, (Liu & Wu, 2019) (Equation 3).

$$S(C_i) = \frac{1}{\text{card}(A_i)} \left| \sum_{a \in A_i} \frac{d\mathcal{L}}{da} \right| \quad (3)$$

However, the information contained in the gradients is often coupled with the activations. The Fisher Information (Theis

et al., 2018) (Equation 4) and 1st order Taylor expansion (Molchanov et al., 2017) (Equation 5) are two notable examples of saliency metrics combining both the information of the activations and their gradients.

$$S(C_i) = \frac{1}{2} \left(\sum_{a \in A_i} a \frac{d\mathcal{L}}{da} \right)^2 \quad (4)$$

$$S(C_i) = \frac{1}{\text{card}(A_i)} \left| \sum_{a \in A_i} a \frac{d\mathcal{L}}{da} \right| \quad (5)$$

2.6. Metric Assumptions

The Fisher Information and 1st Order Taylor expansion are both derived using the Taylor expansion presented in Figure 1. However, they are constructed under very different assumptions. The construction of the Fisher Information (Molchanov et al., 2017) assumes that the gradients of the weights and activations are insignificant. Hence, the 1st order terms in Figure 1 are ignored to derive Equation 4. On the other hand, when using a first-order Taylor expansion, the higher order terms are considered insignificant, leading to this time ignoring the 2nd order terms in Figure 1 to derive Equation 5. These assumptions are typically not simultaneously true for any given network. Moreover, as the pruning process continues, the degree of significance of different components can, and does, change, leading to the invalidation of these implicit assumptions encoded in the choice of saliency metric.

$$\mathcal{L}(A - A_i) - \mathcal{L}(A) \approx \underbrace{\frac{d\mathcal{L}}{dA}(-A_i)}_{\text{1st order terms}} + \underbrace{\frac{1}{2}(-A_i)^T \frac{d^2\mathcal{L}}{dA^2}(-A_i)}_{\text{2nd order terms}}$$

Figure 1: Estimating the effect of pruning the i^{th} output channel of a network with loss function \mathcal{L} using a 2nd-order Taylor development around A , all the activations of the network. A_i is the feature map produced by the i^{th} output channel of the network.

For example, in the case of pruning a partially converged network, the gradients of the weights and activations are very unlikely to be negligible. When pruning a fully converged network, the gradients are much more likely to be negligible. When pruning a fully trained network, we start with converged weights. However, as the pruning process proceeds, we may end up pruning *partially* converged weights, since the pruning process degrades the network.

3. Pruning and Non-Linear Data Dependence

Channel pruning removes the parameters corresponding to output feature maps from a convolutional layer, which can

lead to the removal of more parameters from other layers. In a CNN, the output feature maps of one layer become the input feature maps of the next, introducing a pattern of data dependences in the network graph. This pattern determines which other layers are affected by the pruning of an output feature map from a convolutional layer.

Simple network architectures consist of a linear sequence of layers with feed-forward dataflow, connected head to tail (Figure 2). In this case, the data dependences are purely local. Pruning one output channel causes the corresponding weights in the producer layer to be removed, and also the weights of the corresponding input channel in the consumer (since that channel is now all zeros, these weights can no longer have any effect). However, many popular network architectures have non-linear structure, with more complex data dependence relationships.

To simplify the explanation and illustrations of channel pruning, we do not show the intermediate layers (ReLU, Pooling, Dropout, ...) between convolution layers. Unlike convolutional layers, these layers do not have intra-channel dependencies, and hence do not affect the data dependence structure that we discuss.

In this paper, we refer to the entire set of weights removed due to the removal of the i^{th} output channel (or i^{th} output feature map A_i) of the network as Θ_{C_i} and W_i the output channel weights that are used to produce A_i . Hence, W_i is always a subset of Θ_{C_i} .

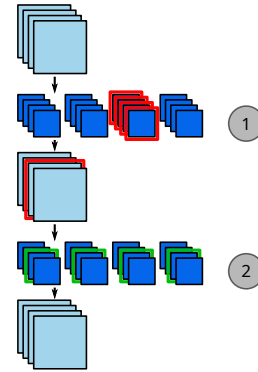


Figure 2: Data dependence structure in convolutional layers. Dark squares are weights, light squares are activations. In our equations, W_i and A_i are the weights and the feature map, respectively (highlighted in red). Θ_{C_i} is the entire set of highlighted parameters. In the figure, convolution layers are labelled by their position in the network, in gray circles.

3.1. Dependence Structure in Group Convolution

For a group convolution with grouping factor, g , C input feature maps, $k \times k$ convolution kernels, and M output feature maps, the weight tensor is of shape $M \times \frac{C}{g} \times k \times k$.

$\frac{C}{g}$ slices of the input feature maps are convolved separately with $\frac{M}{g} \times \frac{C}{g} \times k \times k$ kernels to produce $\frac{M}{g}$ output feature maps. If an input feature map is removed, the corresponding $g - 1$ feature maps also need to be removed to keep the weight tensor dense. Figure 3 shows this constraint.

If we prune the i^{th} local output channel of a convolution layer that has its feature maps consumed by a group convolution with grouping factor g , we must also prune all j^{th} local channels such that $(i - j) \% M/g = 0$ with M the total number of channels produced by the local convolution layer.

Figure 3 shows part of *AlexNet* where we prune the 3rd output channel of Convolution ①. The consumer layer, Convolution ②, is a group convolution with grouping factor 2. Consequently, the 1st output channel of Convolution ① is also pruned, to satisfy the data dependence structure in the graph.

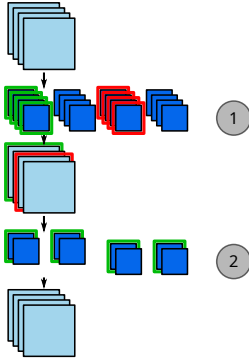


Figure 3: Data dependence structure in AlexNet.

3.2. Dependence Structure with Residual Connections

ResNets contain *residual connections*, which connect multiple layers. When removing an entire channel of weights from the network, the convolutions which consume the pruned feature map need to be resized, as do other convolutions that produce any pruned feature maps.

Figure 4 shows this constraint. Feature maps produced in one block can be fed to multiple convolutions in other blocks through an elementwise addition layer. This leads to a chain of transitive data dependences between multiple subgroups of parameters in convolutions in different blocks, which are not locally connected. In order to satisfy data dependences and maintain a valid dense network, the transitive closure of parameter groups which interact with the pruned feature map also need to be pruned.

4. Proposed Method: The Myopic Oracle

Each saliency metric assigns a saliency value to every group of parameters under consideration. In our case, these are

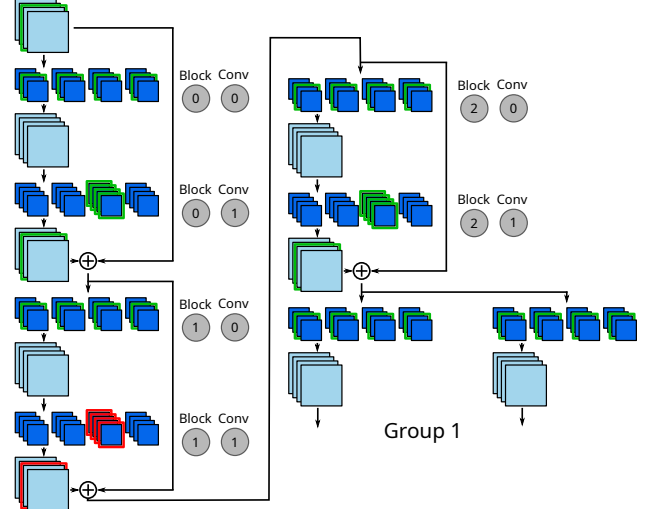


Figure 4: Data dependence structure in ResNet-20

the subsets of parameters in each convolutional layer which correspond to the individual output channels, i.e. parameters which share an M index in the kernel.

If we order these groups of parameters by the magnitude of their saliency value, we can view each of the saliency metrics as a *ranking* of the groups of parameters. To cause least damage to the network, we should remove parameters in order of increasing saliency, so that we prune unimportant parameters first.

Channels are attributed different saliency values (and therefore, likelihood of being pruned) by different saliency metrics. By exploiting these different saliency values we obtain different pruning choices. Ideally, we could combine the best decisions of different saliency metrics. However, the numerical output of different saliency metrics are not directly comparable. For example, the magnitudes of saliency values yielded by taking the mean of the weights may be orders larger than by taking the mean of their gradients.

When different saliency metrics yield different rankings for the parameter groups, we can evaluate which ranking is the closest to reality by performing a direct measurement of the *sensitivity* of the network to the removal of the proposed parameter groups.

For a CNN characterised by the loss function \mathcal{L} and permanent weights Θ , the sensitivity of the i^{th} channel of the network, using the validation set I_{val} is given by the change in the loss caused by replacing all the weights of the i^{th} channel Θ_{C_i} with zeros as given in Equation 6.

$$Sensitivity(C_i) = \mathcal{L}(\Theta - \Theta_{C_i}, I_{val}) - \mathcal{L}(\Theta, I_{val}) \quad (6)$$

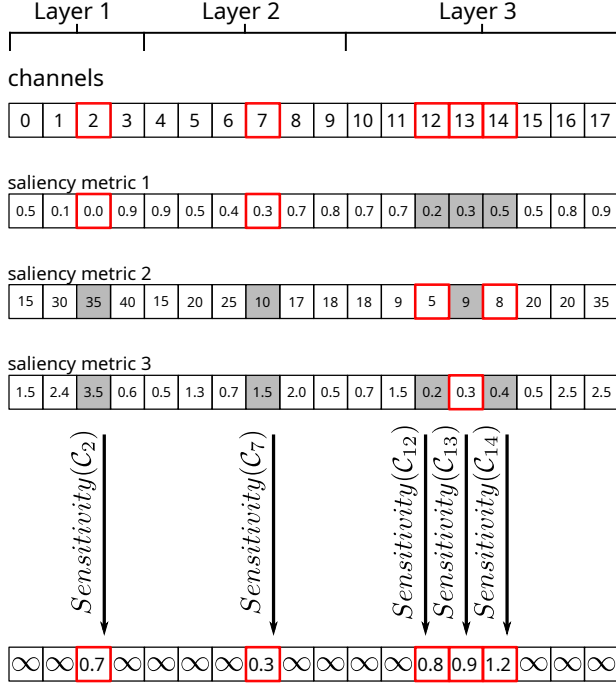


Figure 5: Channel selection with myopic oracle ($k = 5$)

Recall that the “parameters of the i th channel”, Θ_{C_i} , includes weights that are transitively involved in the computation as shown in Figures 2, 3 and 4.

Figure 5 shows an illustration of which channels are selected by the myopic oracle in the case of a pruning scheme with $k = 5$. In the top half of the figure is shown the rankings from each of three constituent saliency metrics.

The myopic oracle visits each of the constituent saliency metrics in a round-robin fashion, and selects the lowest ranked channel to add to the set of channels whose sensitivity should be measured. If the lowest ranked channel has already been selected by another constituent, the second lowest is used instead, and so on. This process continues until k unique channels have been selected. The sensitivity of each channel is then tested, yielding the true ranking of these k channels.

At every pruning step, the myopic oracle measures the sensitivity of only k different channels using the validation set. The choice of k depends on the pruning scheme used. k needs to be at least the number of channels that the pruning scheme considers pruning simultaneously. Hence, k can vary depending on the pruning scheme. The cost of running the myopic oracle for one channel is similar to the cost of computing the dynamic heuristics that use forward passes only. Hence, its cost is not prohibitive but needs to be factored when choosing k .

4.1. Constituent Saliency Metrics

Our composite approach can be used with any saliency metric. Composing all published saliency metrics would be unrealistic. Instead we choose a sample of prominent saliency metrics from the literature that perform well in practice. These metrics rely on different kinds of information. We consider both static and dynamic saliency metrics.

We selected the following constituent saliency metrics to be combined via the myopic oracle. Prior work has shown each of these saliency metrics are very effective.

- Mean of activations (Anwar et al., 2017)
- 1st order Taylor expansion (Molchanov et al., 2017)
- Fisher information (Theis et al., 2018)
- Average of gradients (Liu & Wu, 2019)
- Mean squares of weights (Molchanov et al., 2017)

Even though they are known to perform well, the chosen saliency metrics are constructed under different assumptions and use a diverse selection of parameters from the network. This encourages diversity in the predictions from the composed saliency metric.

5. Experimental Setup

For our experimental setup, we chose a set of constituent saliency metrics to compose via the myopic oracle, and also a general *pruning scheme* to follow. We use the pruning strategy outlined in Algorithm 1 to evaluate the myopic oracle pruning method. We iteratively recompute the channel which should be removed, and remove one channel at a time from the entire network until the test accuracy is degraded beyond a certain threshold (indicated on graphs).

5.1. Pruning Scheme for Saliency Metric Evaluation

Simple pruning schemes rely heavily on the saliency metric’s prediction whereas in sophisticated schemes (He et al., 2018b; Ding et al., 2019; You et al., 2019; Wang et al., 2019), the contribution of the saliency metric can become obfuscated by other factors.

Since our objective is to study the differences in saliency metrics, we chose to eliminate confounding factors by using a simple, iterative pruning scheme without retraining.

Even when retraining is in use, saliency metrics which cause less deviation from the initial test accuracy can lead to less time being spent on retraining, and also to large groups of channels being simultaneously removed, in the case of pruning schemes that allow for simultaneous pruning of

multiple channels. Hence, a good saliency metric reduces the total amount of effort used to find pruned networks.

Algorithm 1 Evaluating different channel selections for a CNN with loss function \mathcal{L} , accuracy \mathcal{Y} and converged weights Θ with K channels for a maximum drop in initial test accuracy of $maxTestAccDrop$

```

initialTestAcc <  $-\mathcal{Y}(\Theta, I_{test})$ 
repeat
   $S(\mathcal{C}_i) = computeSaliency(\mathcal{L}, \Theta, \mathcal{C}_i, I_{val})$  for  $i \in \{1..K\}$ 
  Get  $j$ , such that  $S(\mathcal{C}_j) = \min(S(\mathcal{C}_i))$  for  $i \in \{1..K\}$ 
  and  $\Theta_{\mathcal{C}_j}$  is a non-zero vector.
   $\Theta = \Theta - \Theta_{\mathcal{C}_j}$ 
   $testAcc = \mathcal{Y}(\Theta, I_{test})$ 
until  $testAcc < initialTestAcc - maxTestAccDrop$ 

```

5.1.1. DATASETS

We use the CIFAR-10 dataset in our experiments. As the CIFAR-10 dataset does not inherently contain a validation set, we choose a random subsample of 10000 images from the training set to construct our validation set. We start the pruning process with networks trained using the full training set. Decisions about which channels to remove are made using only the validation set, I_{val} . The performance of the network is evaluated using the test set, I_{test} .

5.1.2. CNN MODELS

LeNet-5(Lecun et al., 1998) and AlexNet(Krizhevsky et al., 2017) are modified so that the first convolutions accept 32×32 RGB input images. ResNet-20(He et al., 2016), NIN(Lin et al., 2013) and the CIFAR10(Krizhevsky, 2009) network are used according to their original descriptions for the CIFAR10 dataset. The networks used are trained from scratch using Caffe(Jia et al., 2014).

Model	TOP-1	#CONV Params
LeNet-5	69%	26.5K
CIFAR10	73%	79.2K
ResNet-20	88%	270K
NIN	88%	966K
AlexNet	84%	2.3M
SqueezeNet	77%	1.23M

Table 1: Summary of trained network accuracy.

5.1.3. EXPERIMENTAL SETUP AND HYPERPARAMETERS

The experiment are run using on a single NVIDIA GTX1080Ti with a batch size of 128 images. We use 80 batches from the test set to measure the reported test ac-

curacies. The base saliency metrics are computed using 2 random batches of the validation set at every pruning step. The myopic oracle also use only 2 random batches of the validation set to evaluate the saliency of its k channels with $k = 16$.

6. Experimental Results and Discussion

Figure 6 presents the result of our experimental evaluation on the five chosen convolutional neural networks. For all five networks, we see that the composite saliency metric matches or exceeds the predictive quality of any of the individual constituent metrics until the test accuracy of the network drops far below useful levels.

We observed the biggest improvement in sparsity ratio for AlexNet and ResNet-20. This can be explained by considering the unique structures of these networks. When removing a channel from these two networks, some additional structural constraints are required to be satisfied to end up with a valid dense network with fewer parameters.

6.1. Behaviour of Composite Metrics

We would like to draw attention to the ResNet-20 (Figure 6a) and NIN (Figure 6b) networks in particular.

For ResNet-20 (Figure 6a), our experiment shows clearly that some saliency metrics are very badly suited for guiding pruning on this network. It is not that these are bad metrics; on the contrary, they perform well on other networks. However, the assumptions baked into these metrics are at odds with the reality of the relationships of the weights, activations, and gradients in ResNet-20, causing them to severely mispredict the effect on the loss function of pruning any individual channel. Using the myopic oracle allows these metrics to be excluded until their assumptions become more in line with the reality of the network structure, instead of causing pathological behaviour if used indiscriminately.

For NIN (Figure 6b), our experiment shows that the composition of metrics via the oracle exhibits smooth, predictable behaviour, where the individual metrics differ dramatically. Even though the individual metrics have such large differences, the composition of the metrics with the oracle is well-behaved, leading to a much less damaging pruning that with any of the metrics individually.

The remainder of the networks exhibit similar behaviour. For CIFAR10 (Figure 6d) and AlexNet (Figure 6e), we see again that the composition of the saliency metrics via the oracle yields a smooth, well-behaved metric, even though the constituent metrics have large differences.

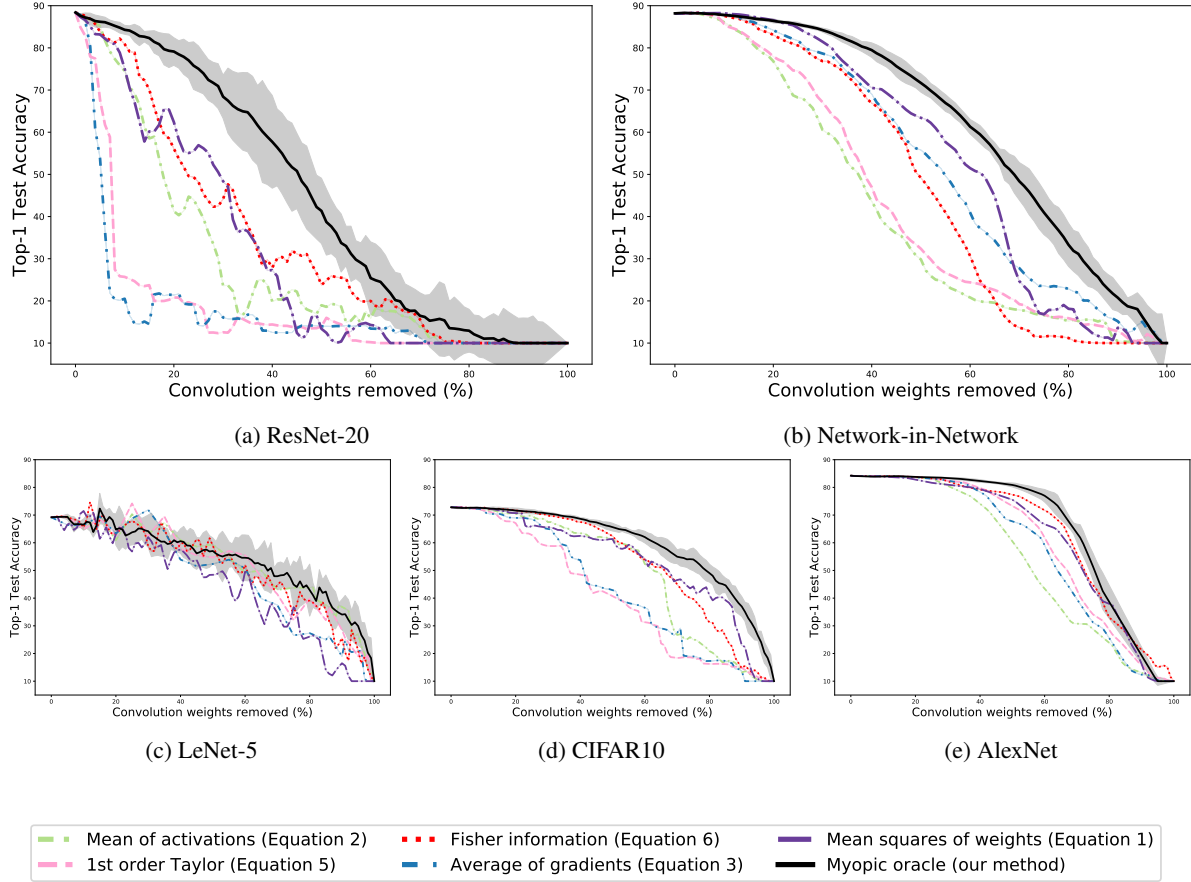


Figure 6: Graphs show TOP-1 test accuracy versus number of convolution weights (%) removed by pruning. Individual saliency metrics are indicated with dashed lines, and the myopic oracle (with $k = 16$) is indicated with a solid line. Error bands for TOP-1 test accuracy for the myopic oracle are shown based on a 95% confidence interval for 8 runs of the experiment.

Saliency Metric	LeNet-5	CIFAR10	ResNet-20	NIN	AlexNet
Mean of activations	25%	30%	6%	14%	33%
1st order Taylor	27%	17%	2%	14%	41%
Fisher information	19%	39%	5%	20%	40%
Average of gradients	29%	26%	2%	22%	39%
Mean squares of weights	7%	24%	4%	27%	40%
Myopic Oracle	$30\% \pm 10$	$43\% \pm 2$	$12\% \pm 3$	$32\% \pm 1$	$55\% \pm 1$

Table 2: Convolution weights removed (%) for a drop in test accuracy of at most 5%.

6.2. Evidence of Phase-Structure in Pruning

Our experimental evaluation demonstrates clearly that there is an emergent *phase structure* in the pruning process, where individual saliency metrics experience phases of high accuracy, and phases of lower accuracy.

Taking ResNet-20 (Figure 6a) as an example, and looking

at the first half of the pruning process, we can clearly see that individual saliency metrics experience phases where they are presenting the best pruning candidates, and phases where they are not. Some metrics even exchange the top spot repeatedly as the pruning process continues.

This structure is apparent in all of our experiments, but is most clearly defined in ResNet-20, and in CIFAR10 (Fig-

ure 6d). Although in hindsight we can see that it would be beneficial to switch saliency metrics at these crossover points, without performing an evaluation of sensitivity, it is not possible to know exactly when one should switch metrics, nor to identify to which metric one should switch. The myopic oracle provides an exceptionally straightforward and effective solution to this problem, which introduces no constraints on the actual saliency metrics being combined.

6.3. Quality of Pruned Networks

Table 2 summarizes the level of pruning achieved in our experiments for a maximum reduction of 5% points in Top-1 test accuracy.

Using the myopic oracle to compose existing saliency metrics yields a composite metric which makes better pruning decisions than any of the individual metrics which were composed. The myopic oracle consistently selects channels to prune that result in a smaller loss in test accuracy. We also present the proportion of weights removed for the constituent saliency metrics, if used exclusively, as in prior work. The composed metric achieves better sparsity ratios for a given drop in test accuracy than using any single metric throughout.

On every network, our approach meets or exceeds the performance of all the state of the art saliency metrics used individually. The best results are seen on ResNet-20, where fully twice as many weights can be removed using our approach versus the next-best individual saliency metric.

7. Conclusion

Many different pruning saliency metrics have been proposed, and on average most metrics make good choices most of the time. However, no metric is perfect, and all metrics make really poor choices from time to time. Ideally, it would be possible to combine the best selections from several metrics, but the values produced by different saliency metrics are not comparable.

We propose a method to compose different saliency metrics using a myopic oracle. We identify the lowest ranked channel(s) from each of several different saliency metrics. Our myopic oracle then evaluates the sensitivity with respect to removing the proposed channels. The sensitivity measures the impact on cross-entropy loss when performing forward passes with one or more mini-batches. The sensitivity provides a single comparable measurement that can be used to compose and rank the results of the best existing saliency measures.

A very large number of different pruning schemes have been proposed in the literature. These include different interactions of pruning and retraining, different schedules to

decide how many channels should be pruned at each stage, selecting channels from within one layer or across multiple layers, and approaches that allow pruned channels to be reinstated at a later stage. To achieve a fair comparison of different saliency metrics, we evaluate each metric within a simple, regular pruning scheme.

We find that our method of composing multiple saliency metrics significantly outperforms individual metrics. The myopic oracle consistently selects channels that result in a smaller loss in test accuracy. By choosing the best from several different metrics, we avoid the occasional poor choices that arise from even the most advanced saliency metrics. Our method can be used to improve the performance of any set of existing pruning saliency metrics, and advances the state of the art in identifying unnecessary or redundant sets of neural network parameters.

References

- Anwar, S., Hwang, K., and Sung, W. Structured pruning of deep convolutional neural networks. *JETC*, 13(3): 32:1–32:18, 2017.
- Ding, X., Ding, G., Guo, Y., Han, J., and Yan, C. Approximated oracle filter pruning for destructive CNN width optimization. In *Proceedings of the 36th International Conference on Machine Learning, ICML 2019, 9-15 June 2019, Long Beach, California, USA*, volume 97 of *Proceedings of Machine Learning Research*, pp. 1607–1616. PMLR, 2019. URL <http://proceedings.mlr.press/v97/ding19a.html>.
- Frankle, J. and Carbin, M. The lottery ticket hypothesis: Finding sparse, trainable neural networks. In *ICLR*, 2019.
- Han, S., Pool, J., Tran, J., and Dally, W. J. Learning both weights and connections for efficient neural network. In *NIPS*, pp. 1135–1143, 2015.
- Hassibi, B. and Stork, D. G. Second order derivatives for network pruning: Optimal brain surgeon. In *NIPS*, pp. 164–171. Morgan Kaufmann, 1992.
- He, K., Zhang, X., Ren, S., and Sun, J. Deep residual learning for image recognition. In *2016 IEEE Conference on Computer Vision and Pattern Recognition, CVPR 2016, Las Vegas, NV, USA, June 27-30, 2016*, pp. 770–778, 2016. doi: 10.1109/CVPR.2016.90. URL <https://doi.org/10.1109/CVPR.2016.90>.
- He, Y., Kang, G., Dong, X., Fu, Y., and Yang, Y. Soft filter pruning for accelerating deep convolutional neural networks. In *IJCAI*, pp. 2234–2240. ijcai.org, 2018a.
- He, Y., Lin, J., Liu, Z., Wang, H., Li, L., and Han, S. AMC: automl for model compression and acceleration on mobile devices. In *ECCV (7)*, volume 11211 of *Lecture Notes in Computer Science*, pp. 815–832. Springer, 2018b.
- Hu, H., Peng, R., Tai, Y., and Tang, C. Network trimming: A data-driven neuron pruning approach towards efficient deep architectures. *CoRR*, abs/1607.03250, 2016. URL <http://arxiv.org/abs/1607.03250>.
- Jia, Y., Shelhamer, E., Donahue, J., Karayev, S., Long, J., Girshick, R., Guadarrama, S., and Darrell, T. Caffe: Convolutional architecture for fast feature embedding. *arXiv preprint arXiv:1408.5093*, 2014.
- Karnin, E. D. A simple procedure for pruning back-propagation trained neural networks. *IEEE Trans. Neural Networks*, 1(2):239–242, 1990.
- Krizhevsky, A. Learning multiple layers of features from tiny images, 2009. URL <https://www.cs.toronto.edu/~kriz/cifar.html>.
- Krizhevsky, A., Sutskever, I., and Hinton, G. E. ImageNet classification with deep convolutional neural networks. *Commun. ACM*, 60(6):84–90, 2017. doi: 10.1145/3065386. URL <http://doi.acm.org/10.1145/3065386>.
- Lebedev, V. and Lempitsky, V. S. Fast convnets using group-wise brain damage. In *CVPR*, pp. 2554–2564. IEEE Computer Society, 2016.
- LeCun, Y., Denker, J. S., and Solla, S. A. Optimal brain damage. In *Advances in Neural Information Processing Systems 2, [NIPS Conference, Denver, Colorado, USA, November 27-30, 1989]*, pp. 598–605, 1989. URL <http://papers.nips.cc/paper/250-optimal-brain-damage>.
- Lecun, Y., Bottou, L., Bengio, Y., and Haffner, P. Gradient-based learning applied to document recognition. In *Proceedings of the IEEE*, volume 86, pp. 2278–2324, November 1998. doi: 10.1109/5.726791.
- Lee, N., Ajanthan, T., and Torr, P. H. S. Snip: single-shot network pruning based on connection sensitivity. In *7th International Conference on Learning Representations, ICLR 2019, New Orleans, LA, USA, May 6-9, 2019*, 2019. URL <https://openreview.net/forum?id=B1VZqjAcYX>.
- Li, H., Kadav, A., Durdanovic, I., Samet, H., and Graf, H. P. Pruning filters for efficient convnets. In *ICLR*, 2017.
- Lin, M., Chen, Q., and Yan, S. Network in network. *CoRR*, abs/1312.4400, 2013. URL <http://arxiv.org/abs/1312.4400>.
- Liu, C. and Wu, H. Channel pruning based on mean gradient for accelerating convolutional neural networks. *Signal Processing*, 156:84 – 91, 2019. ISSN 0165-1684. doi: <https://doi.org/10.1016/j.sigpro.2018.10.019>. URL <http://www.sciencedirect.com/science/article/pii/S0165168418303517>.
- Mao, H., Han, S., Pool, J., Li, W., Liu, X., Wang, Y., and Dally, W. J. Exploring the granularity of sparsity in convolutional neural networks. In *2017 IEEE Conference on Computer Vision and Pattern Recognition Workshops (CVPRW)*, pp. 1927–1934, July 2017. doi: 10.1109/CVPRW.2017.241.
- Molchanov, P., Tyree, S., Karras, T., Aila, T., and Kautz, J. Pruning convolutional neural networks for resource efficient inference. In *ICLR*, 2017.
- Mozier, M. and Smolensky, P. Skeletonization: A technique for trimming the fat from a network via relevance assessment. In *NIPS*, pp. 107–115. Morgan Kaufmann, 1988.

- Polyak, A. and Wolf, L. Channel-level acceleration of deep face representations. *IEEE Access*, 3:2163–2175, 2015.
- Reed, R. Pruning algorithms-a survey. *IEEE Trans. Neural Networks*, 4(5):740–747, 1993. doi: 10.1109/72.248452. URL <https://doi.org/10.1109/72.248452>.
- Theis, L., Korshunova, I., Tejani, A., and Huszár, F. Faster gaze prediction with dense networks and Fisher pruning. *CoRR*, abs/1801.05787, 2018.
- Wang, Z., Li, C., Wang, X., and Wang, D. Towards efficient convolutional neural networks through low-error filter saliency estimation. In Nayak, A. C. and Sharma, A. (eds.), *PRICAI 2019: Trends in Artificial Intelligence - 16th Pacific Rim International Conference on Artificial Intelligence, Cuvu, Yanuca Island, Fiji, August 26-30, 2019, Proceedings, Part II*, volume 11671 of *Lecture Notes in Computer Science*, pp. 255–267. Springer, 2019. doi: 10.1007/978-3-030-29911-8_20. URL https://doi.org/10.1007/978-3-030-29911-8_20.
- Wen, W., Wu, C., Wang, Y., Chen, Y., and Li, H. Learning structured sparsity in deep neural networks. In *NIPS*, pp. 2074–2082, 2016.
- You, Z., Yan, K., Ye, J., Ma, M., and Wang, P. Gate decorator: Global filter pruning method for accelerating deep convolutional neural networks. In *Advances in Neural Information Processing Systems 32: Annual Conference on Neural Information Processing Systems 2019, NeurIPS 2019, 8-14 December 2019, Vancouver, BC, Canada*, pp. 2130–2141, 2019. URL <http://papers.nips.cc/paper/8486-gate-decorator-global-filter-pruning-method-for-accelerating-deep-convolutional-neural-networks>.